Fluorine directed two-dimensional cruciform π-π stacking in diketopyrrolopyrroles

Jesus Calvo-Castro,[c] Graeme Morris,[a] Alan R. Kennedy,[b] and Callum J. McHugh*[a]*

[a] School of Science and Sport, University of the West of Scotland, Paisley, PA1 2BE, UK.

[b] Department of Pure & Applied Chemistry, University of Strathclyde, Glasgow, G1 1XL, UK.

[c] School of Life and Medical Sciences, University of Hertfordshire, Hatfield, AL10 9AB, UK.

*Corresponding authors: j.calvo-castro@herts.ac.uk, callum.mchugh@uws.ac.uk

ABSTRACT: Enhanced bulk dimensionality in organic materials employed in optoelectronic devices is desirable and can overcome fabrication issues related to structural defects and grain boundaries. Herein, we report a novel fluorinated diketopyrrolopyrrole single crystal structure, which displays a unique, mutually orthogonal, 2-dimensional cruciform π-π stacking arrangement. The crystal structure is characterised by an unusually large number of nearest neighbour dimer pairs which contribute to a greater thermal integrity than structurally analogous equivalents. Binding energies and charge transfer integrals were computed for all of the crystal

extracted dimer pairs by means of M06-2X density functional at 6-311G(d) level. Although weak, a number of intermolecular interactions involving organic fluorine (C-F---H, π_F---π and C-F---π_F) were identified to influence the supramolecular assembly of these dimer pairs. Charge transfer integrals for the two π-π stacking crystal dimers were determined using the energy splitting in dimer method. Ambipolar charge transport favouring electron transfer approaching that of rubrene is predicted in both of these π-π stacks with a greater magnitude of coupling observed from those dimers perpetuating along the crystallographic *a*-axis. Charge transport behaviour in the single crystal is greatly influenced by selective fluorination of the N-benzyl substituents and is consistent with the crystal extracted π-π stacking dimer geometries and their overall influence on wavefunction overlap. The reported structure is an interesting electron transport material that could be exploited, particularly in thin film based optoelectronic devices, where high bulk dimensionality is required.

INTRODUCTION

The concept of dimensionality is widely employed to describe both molecular and bulk structural properties in organic semiconductors.[1,2] High bulk dimensionality is proposed to be advantageous, overcoming significant fabrication issues relating to structural defects and grain boundaries in charge mediating devices. It is accepted that linear conjugated systems often display the most efficient bulk assemblies for charge transport based on 1-dimensional π-π stacking with high electronic coupling and transfer integrals. These systems are often surpassed in device performance however, by molecular scaffolds displaying more effective solid state aggregation and a greater number of electronic interactions that consist of 2-dimensional or 3-dimensional π-π stacking in mutually orthogonal directions.[1]

Many examples of conjugated π-systems that exhibit higher orders of molecular and bulk dimensionality have been reported, including the archetypal swivel and spiro-centred oligothiophene cruciforms, perylenediimides, TIPS pentacene cruciforms, dinapththothiophenes, benzobisthiazoles and tetrathiafulvalene analogues.[1-3] Recent developments in this area have focused on the design of non-linear molecular architectures based on star-shaped π-conjugated platforms. Whilst several of these systems display unique and useful solid state properties, they are often limited by a propensity to form amorphous morphologies in the bulk state.[1,4] Clearly, there is a strong rationale to design new, improved molecular architectures that facilitate efficient conjugation coupled with predictable, controllable and crystalline solid state behaviour.

First reported in 1974,[5] diketopyrrolopyrroles (DPPs) are ubiquitously employed in industry as high performance organic pigments, owing to their highly desirable colouristic and fastness properties.[6-11] More recently, materials based upon DPPs have attracted interest as promising

charge transfer mediating materials in optoelectronic devices such as organic light emitting diodes, organic field effect transistors and organic photovoltaics for solar energy conversion.[12-27] The concept of enhanced dimensionality in DPP containing architectures has been reported, although this has focused mainly on an increase in molecular dimensionality based around linear conjugated and non-conjugated systems.[28] In star-shaped molecules such as those described, strong quadrupole based aggregation in the solid state limits charge carrier performance in field effect transistor applications. One potential strategy to improve charge transport behaviour in such star-shaped environments is through the correct choice and position of the solubilising N-substituents, aimed to direct more efficient solid state interactions.[1]

We are engaged in the rational design and systematic engineering of crystalline and thin film architectures based upon N-substituted DPPs[29-34] and have recently demonstrated in a number of systems that small structural variations can systematically influence and control the packing motifs via manipulation of their single crystal intermolecular interactions.[29-32] We are specifically interested in the dramatic changes observed to intermonomer displacements in crystal derived π-π stacking dimer pairs in these systems, which are reported to play a crucial role in determining the charge transfer properties of organic semiconductors.[29-32,35-37] We have shown that N-benzylation is an effective strategy in the molecular design of DPPs, with N-benzyl substituted single crystal examples characterised by close alignment along their short molecular axis with the emergence of slipped cofacial 1-dimensional π-π stacks[29-32] unlike their pigment and alkylated counterparts.[38-41] This close intermonomer alignment along the short molecular axis in N-benzyl DPP architectures is associated to larger computed intermolecular interactions which are desirable for the enhancement of π-π stacking thermal integrity and to

furthermore maximise wavefunction overlap, critical in optimising hole and electron transfer behaviour.

In addition, halogen substitutions have been widely explored in π-conjugated organic semiconductors and we have shown that they play an active role in determining the solid state behaviour in N-benzyl DPPs. Fluorine substitution of hydrogen is often employed in the life sciences and solid state chemistry[42-53] in light of their similar polarizabilities, with substantial change in their occupied volume. Physical and chemical properties in comparative systems are influenced by the significant variation in electronegativity, such as the reversal of the electron density when comparing perfluorinated rings and their non-fluorinated analogues and is often associated to the appearance of an array of intermolecular interactions such as C-F---H, C-F---F-C, C-F---π_F, π_F---π and π_F---π_F contacts.[44,45,49-52] Hydrogen bonding interactions involving organic fluorine are rarely encountered despite its high electronegativity and is related to the low polarisability of this atom.[44,45,54] We have previously reported that isosteric fluorine substitution in N-benzyl substituted DPPs plays an important role in determining solid state packing behaviour and can be tuned to access unique structural motifs.[29] The π-π stacking regime of crystal structures bearing direct fluorination of the DPP core phenyl rings and benzyl groups display the now characteristic 1-dimensional slipped π-π stacking motif arising from N-benzyl substitution, with the degree of long and short molecular axes slip controlled by the position of fluorine substitution. Surprisingly, this type of stacking behaviour is diminished completely by trifluoromethyl substitution at the para position of the core phenyl rings, leading to novel packing motifs underpinned by an orthogonal orientation of the π-π stacking dimer pairs and formation of a non-covalent organic framework characterised by well-defined channels perpetuating along the length of a single crystallographic axis.[29]

In all of the DPP crystal structures reported to date by our group, π-π stacking behaviour has been 1-dimensional in the bulk state, despite the star-shaped structure of the molecular building blocks involved. In the following study, we extend our earlier work on fluorine substitution in DPPs and report the synthesis and characterisation of a novel symmetrical fluorine substituted N-benzyl DPP single crystal structure, which surprisingly, exhibits 2-dimensional π-π stacking (Scheme 1). This new structure, ***HHFBDPP***, was given a name in the form of ***XYZBDPP***, in line with our previously reported series[29] for ease of comparison throughout the present study, where **X** and **Y** denote the substitution on the para and meta positions of DPP core phenyl rings respectively. In turn, **Z** denotes isosteric substitution of the phenylic atoms for fluorine atoms within the benzyl groups.

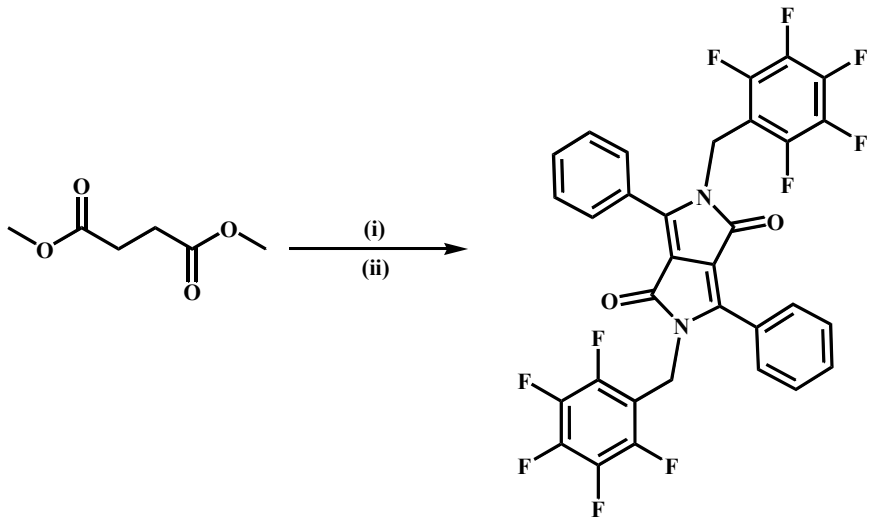

Scheme 1. ***HHFBDPP*** synthetic route. (i) PhCN, Na, t-amyl alcohol, reflux; (ii) Pentafluoro-BnBr, K_2CO_3, DMF, 120 °C;

The crystal structure of ***HHFBDPP*** exhibits a greater number of nearest neighbour dimer pairs (vide infra) when compared to all previous DPP based systems examined by us[29-31] and more importantly all of its dimer pairs are centrosymmetric, facilitating a theoretical determination of their charge transfer properties via the energy splitting in dimer method. Two separate dimer pairs were observed to form one-dimensional π-π stacking motifs and their respective π-π dimer stacking arrangements are illustrated in Figure 1. The first of these two π-π dimer pairs (dimer pair II) exhibits the characteristic[29-31] slipped-cofacial intermonomer arrangement associated with N-benzyl substitution, with a large displacement along the long molecular axis (Δx = 9.13 Å) and a shift along the short molecular axis (Δy = 1.64 Å), consistent with that reported by us previously for the meta fluorinated analogue, ***HFFBDPP*** (Δx and Δy = 9.12 and 2.31 Å respectively).[29] The latter reinforced our conclusion that isosteric fluorine substitution of the benzyl phenylic hydrogen atoms leads to larger displacements along the long and short molecular axes than those exhibited by non-fluorinated equivalents, such as ***HHHBDPP*** (where Δx and Δy = 4.52 and 0.05 Å respectively).[30] The second stacking interaction based on dimer pair (V) of ***HHFBDPP*** is characterised by unusual intermonomer displacements (Δx = 0.58 and Δy = 4.43 Å) which are much more in line with those observed for non N-substituted DPP pigments. To the best of our knowledge, the crystal structure of ***HHFBDPP*** represents the first N-substituted DPP derivative to exhibit such a large displacement along the short molecular axis in a π-π stacking interaction. In addition, π-π stacking dimer pairs II and V extend into mutually orthogonal one-dimensional π-π slipped cofacial stacking motifs running parallel to the *b* and *a* crystallographic axes respectively. This cruciform arrangement of π-π stacking interactions is unique and ***HHFBDPP*** represents the first example of a DPP where high order bulk dimensionality is observed in the single crystal structure. In the following report, the nature of

the computed binding energies and charge transfer properties of these distinctive stacking assemblies will be discussed.

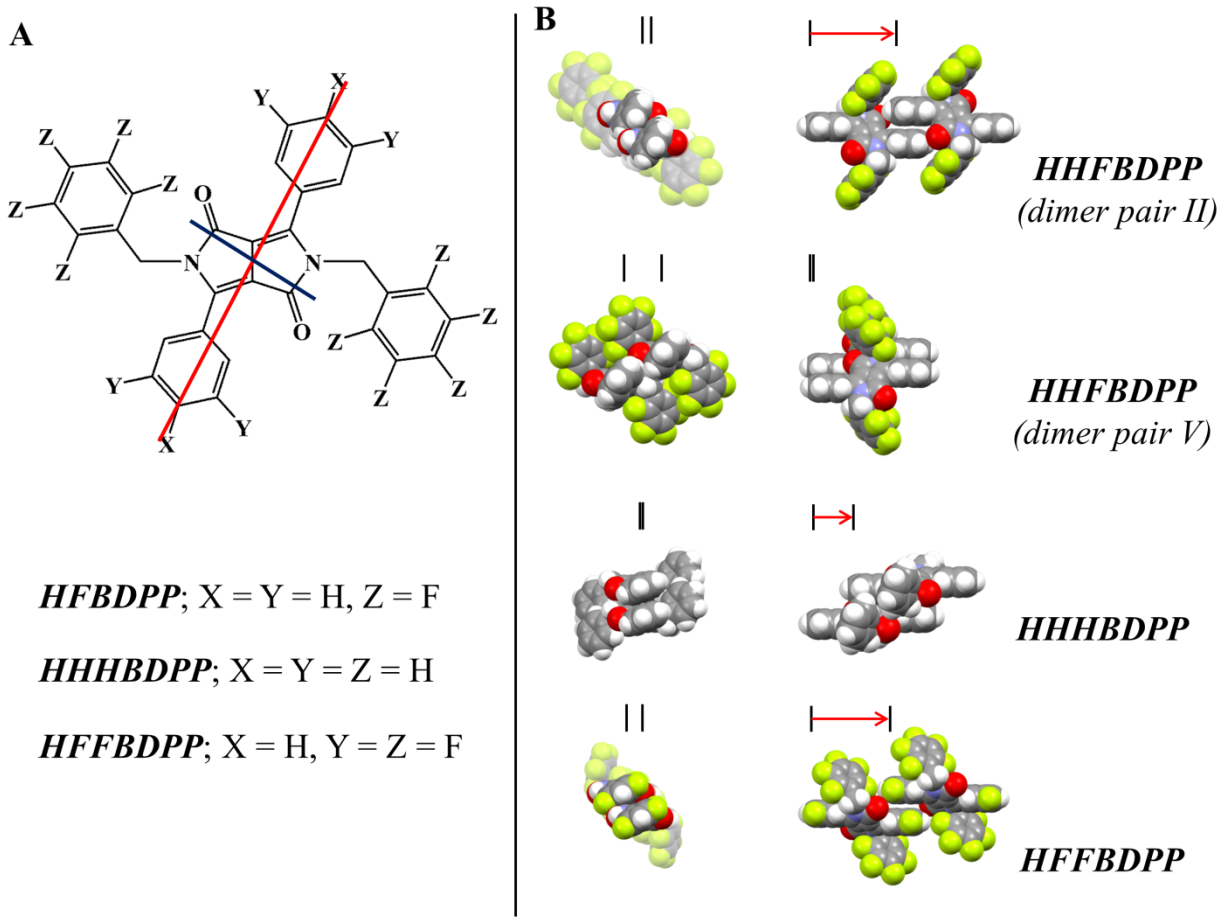

Figure 1. **A** Illustration of long and short molecular axes in DPP-based architectures. **B** Long and short molecular axis view of π-π dimer pair II and V of ***HHFBDPP*** and analogous systems, ***HHHBDPP*** and ***HFFBDPP*** for comparison. Phenyl-DPP cores in short molecular axis views of ***HHFBDPP*** and ***HFFBDPP*** are highlighted for ease of visualisation.

EXPERIMENTAL SECTION

Reagents and instrumentation. Unless otherwise specified, all starting materials and reagents were purchased from Fisher Scientific, Sigma-Aldrich or VWR and used as received without further purification. ^{1}H NMR and ^{13}C NMR spectra were determined using a Bruker AV3 400 MHz spectrometer (in $CDCl_3$). Elemental analyses were carried out using the service provided at the University of Strathclyde in Glasgow, UK. FTIR analyses were carried out on the neat samples by attenuated total reflectance using a Thermo Scientific Nicolet iS5 FTIR Spectrometer, with an iD5 ATR (Diamond) sampling accessory.

Synthesis.

2,5-bis(pentafluorobenzyl)-3,6-diphenylpyrrolo[3,4-c]pyrrole-1,4-dione (*HHFBDPP*). A suspension of 3,6-diphenyldihydropyrrolo[3,4-c]pyrrole-1,4-dione[30] (0.58 g, 2.01 mmol) and anhydrous K_2CO_3 (0.32 g, 2.32 mmol) in anhydrous DMF (50 mL) was heated at 120 °C under nitrogen atmosphere. At this temperature and under vigorous stirring a solution of 2,3,4,5,6-pentafluorobenzyl bromide (0.57 g, 2.18 mmol) in DMF (30 mL) was added over 1 h. Stirring and heating at 120 °C were continued for 1 h and after cooling to room temperature the crude product was purified by wet flash chromatography eluting with hexane-dichloromethane (3:7) and then precipitated with methanol to give ***HHFBDPP*** (0.179 g, 25.3 %) as a bright yellow powder. ^{1}H NMR (CDCl3): 5.07 (4H, s, CH_2); 7.50-7.55 (6H, m, ArH), 7.66-7.71 (4H, m, ArH). ^{13}CNMR ($CDCl_3$): 34.42, 109.78, 127.43, 128.46, 129.11, 131.54, 148.24, 161.86. IR (ATR)/cm^{-1}: 3065 (ArH), 2959 (CH_2), 1680 (C=O), 1503 (C=C), 1378 (CH_2), 1352 (CH_2), 1123 (CF), 1017 (CF), 789 (ArH). Anal. Calcd. for $C_{32}H_{14}F_{10}N_2O_2$: C, 59.27; H, 2.18; N, 4.32. Found:

C, 58.45; H, 1.85; N, 4.18. TLC: Rf (dichloromethane) 0.41, (ethyl acetate) 0.83. Melting Point: 307-310 °C

Preparation of Crystal for Single Crystal X-Ray Diffraction analysis. The single crystal of ***HHFBDPP*** was obtained from DCM/hexane (1:1) by slow evaporation of a cooled solution.

Crystal structure determination. Crystallographic measurements were made with an Oxford Diffraction Gemini S instrument at 123 K using Cu (λ = 1.5428 Å) graphite monochromated radiation. The structure was refined against F^2 and against all unique reflections to convergence using SHELX-97.[55] Selected crystallographic and refinement parameters are; $C_{32}H_{14}F_{10}N_2O_2$, triclinic $P\bar{1}$; a = 5.9851(4), b = 9.7414(5), c = 11.0925(6) Å, α = 94.842(4), β = 101.453(5), γ = 92.320(5) °, V = 630.50(6) Å^3, Z = 1, Z' = 0.5; reflections collected 7311, reflections unique 2488, R_{int} = 0.0393, $2\theta_{max}$ = 146.2 °; For 208 parameters, R = 0.0435 (F for 2121 observed reflections), R_w = 0.1268 (F^2 all unique reflections), S = 1.050. Selected parameters are given in Table 1 and full details are given in the deposited cif files. CCDC reference number 1481505 contains the supplementary crystallographic data for this paper.

Computational details. Using a cut-off distance of van-der-Waals (vdW) radius + 0.3 Å, all nearest neighbouring dimer pairs derived from the experimentally determined crystal structure of ***HHFBDPP*** were identified and their intermolecular interactions and charge transfer integrals computed. Dimer pair binding energies, ΔE_{CP}, were all corrected for Basis Set Superposition Error (BSSE) using the counterpoise method of Boys and Bernardi.[56] Transfer integrals for holes (t_h) and electrons (t_e) were computed within the framework of the energy splitting in dimer method where t_h and t_e are given by half the splitting between the dimer HOMO/HOMO(-1) and LUMO/LUMO(+1) orbitals respectively.[35] All molecular modelling studies in this work were

carried out using Truhlar's density functional M06-2X[57] at the 6-311G(d) level as implemented in Spartan10[58] software unless otherwise stated. This density functional has been shown to give a good account of the dimer interactions of π-conjugated systems.[37,59]

RESULTS AND DISCUSSION

Structural description. As is common for related structures,[29,30,32] the molecular structure of ***HHFBDPP*** has crystallographically imposed *i* symmetry (Z' = 0.5) with the centre of symmetry lying in the middle of the C1-C1' bond. This necessitates an *anti*-conformation with the C_6F_5 groups lying above and below the plane of the DPP ring. Previous structures in this family have been described as π-π stacks with a continuum of structures with different degrees of slip along the long molecular axis.[29-32] Small degrees of slip correspond to close contacts between the DPP rings and the (non-benzyl) C_6X_5 rings whilst larger degrees of slip correspond to contacts between pairs of C_6X_5 rings. ***HHFBDPP*** has a structure that fits into this continuum albeit with a large long axis slip that is most similar to the series' previously described end member HFFBDPP. The centroid to centroid distance between the phenyl rings is 3.792 Å and so like ***HFFBDPP*** this is a relatively long contact that lies outside the contact distance of van der Waals interactions. With respect to van der Waals distances, the shortest contacts are π-π interactions between the fluorinated rings (shortest C…C distance 3.293(2) Å), F…F contacts (shortest 2.787(2) Å) and non-classical and weak hydrogen bonds between the C=O group and H atoms of the phenyl rings (shortest H…O 2.42 Å).

Intermolecular interaction energies, ΔE_{CP}. Control over the substitution effects in π-conjugated organic crystalline materials and rationalising the nature of intermolecular interactions and packing motifs still represents a major challenge in supramolecular design. In

order to broaden our understanding of isosteric fluorine substitution in N-benzyl substituted DPPs, all of the nearest neighbour dimer pairs within a distance of van der Waals + 0.3 Å were identified for ***HHFBDPP*** and their intermolecular interactions computed, with emphasis placed on the identification of fluorine directed stabilisation. Organic fluorine has been extensively reported to promote a number of different types of intermolecular interactions such as C-F---H, C-F---F-C, C-F---π_F, π---π_F and π_F---π_F[44,45,49-53] which although are normally observed to be weak can play a substantial role in determining packing motifs.

The large number of nearest neighbour dimer pairs (16) observed for ***HHFBDPP*** (site positions reported in SI 1), contrasts to those described by us previously for analogous systems such as ***HHHBDPP***[30] (12) and ***HFFBDPP***[29] (10). Each of the dimer pairs in ***HHFBDPP*** were identified to be centrosymmetric with identical site energies, which is consistent with the non-fluorinated analogue, ***HHHBDPP***.[30] The experimentally determined melting point of 307-310 °C for the single crystal of ***HHFBDPP*** was observed to exceed those reported by us previously for single crystals of the structural analogues ***HHHBDPP*** and ***HFFBDPP*** (278 °C and 268-270 °C respectively),[29,30] consistent with the number of nearest neighbour dimer pairs in each (16, 12 and 10 respectively) and crudely represented by the sum of the computed intermolecular interactions for each systems (ΔE_{CP}^{tot} = -299.0 kJ mol^{-1}, -294.7 kJ mol^{-1} and -241.9 kJ mol^{-1} respectively). It is apparent that substitutions carried out on the DPP core phenyl rings in fluorinated systems are responsible for a decrease in the thermal integrity of their respective single crystals, with benzyl fluorination in this case actually enhancing thermal stability.

In light of the crucial role played by π-π stacking motifs in determining the charge transport properties of organic conjugated materials,[35-37] it is significant that two of the identified dimer pairs of ***HHFBDPP*** (dimer pairs II and V) exhibit such a stacking assembly (Figure 2). Dimer

pair II is characterised by the slipped cofacial π-π stacking motif observed previously in N-benzyl substituted DPPs, where the displacement along the long and short molecular axes (see Figure 1) are observed to be analogous to those for the meta-fluorinated analogue, ***HFFBDPP*** (Δx of 9.13 and 9.12 and Δy of 1.64 and 2.31 Å for ***HHFBDPP*** and ***HFFBDPP*** respectively).[29,30] These observed displacements along the short molecular axis reinforce our previous findings that intermonomer overlap is significantly diminished upon isosteric fluorine substitution of the phenylic hydrogen atoms within the benzyl groups and results in larger shifts not found in the non-fluorinated equivalent, ***HHHBDPP*** (Δx = 4.52 and Δy = 0.05 Å).[30] The other π-π stacking dimer (pair V of ***HHFBDPP***) is characterised by displacements along the long and short molecular axes (Δx and Δy = 0.58 and 4.43 Å respectively),[29] which are much more consistent with pigment analogues,[39-41] non-substituted acenes and thiophenes.[60-63] From a search of the Cambridge Structural Database (CSD) this is the first reported non N-substituted DPP structure to display such a displaced cofacial π-π stacking interaction along the short molecular axis.

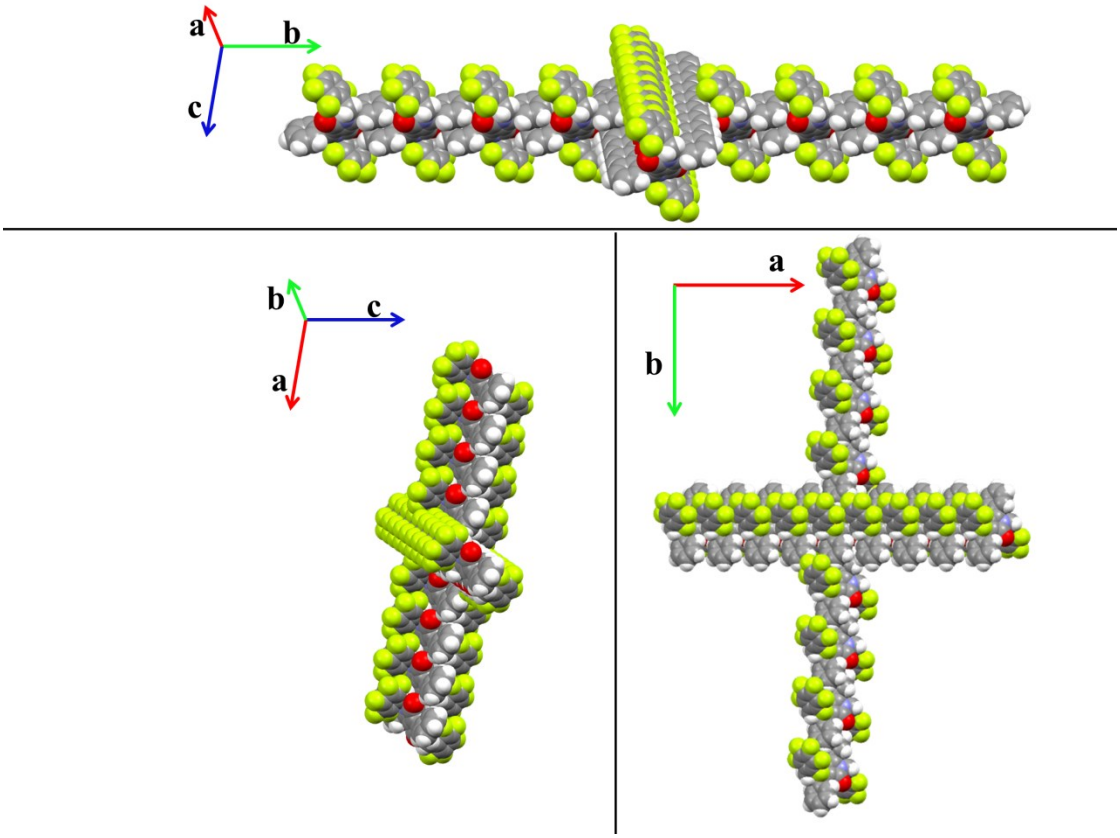

Figure 2. Illustration of the cruciform supramolecular arrangement observed in ***HHFBDPP***.

Figure 2 illustrates the unique supramolecular arrangement of π-π stacking observed in ***HHFBDPP***, where dimer pairs II and V pairs form mutually orthogonal one-dimensional π-π slipped cofacial stacking motifs that perpetuate the length of the *b* and *a* crystallographic axes respectively. The supramolecular assembly of both π-π stacking domains affords a cruciform arrangement in the bulk which is highly advantageous in organic semiconductors. In addition, the π-π stacking dimer pairs II and V were observed to exhibit the largest computed intermolecular interaction energies from all of those identified in the single crystal structure of ***HHFBDPP*** (see Table 2). For dimer pair II, which exhibits a closer alignment along the short molecular axis than dimer pair V (Δy = 1.64 and 4.43 Å for dimer pairs II and V respectively), an intermolecular interaction energy of -41.08 kJ mol^{-1} was computed. This is lower than that

computed for the π-π stacking dimer pair of the non-fluorinated equivalent, ***HHHBDPP*** for which we reported ΔE_{CP} of -70.20 kJ mol^{-1},[30] but greater than that computed for the analogue bearing fluorine substituents on the benzyl phenyl rings and at the meta positions of the DPP core phenyl rings (***HFFBDPP***, where ΔE_{CP} = -22.46 kJ mol^{-1}).[29] We associate the differences in interaction energies of the respective π-π stacks to the interactions facilitated by their different displacements along the long and short molecular axes, as illustrated in Figure 1 (Δx/Δy = 4.52/0.05, 9.13/1.64 and 9.12/2.31 Å for ***HHHBDPP***, ***HHFBDPP*** and ***HFFBDPP*** respectively). In turn, a larger computed binding energy of -56.17 kJ mol^{-1} was determined for the π-π stacking dimer pair V of ***HHFBDPP*** which we similarly ascribe to the closer intermonomer alignment observed for this dimer pair along the long molecular axis (Δx = 9.13 and 0.58 Å for dimer pairs II and V respectively) and therefore more favourable intermolecular interactions. Both π-π stacking dimer pairs of ***HHFBDPP*** were observed to exhibit greater binding energies than those computed for the cofacial π-π dimer pair identified in the single crystal structure of rubrene (ΔE_{CP} = -35.60 kJ mol^{-1} using M06-2X/6-311G*), which is an archetypal material widely employed as a charge transfer mediator in optoelectronic devices.[36,64,65] Therefore, we anticipate a greater thermal integrity of the two π-π stacking dimer assemblies reported for ***HHFBDPP***; a property which is highly desirable in light of the sensitivity (vide infra) of computed charge transfer integrals to small intermonomeric displacements.[29-31,37,62,66] Given the importance of intermolecular interactions in promoting or precluding certain supramolecular frameworks, we computed the binding energies for all of the dimer pairs identified for ***HHFBDPP*** in order to broaden our understanding of non-covalent interactions in fluorine containing N-benzyl DPPs and their role in defining such supramolecular architectures.

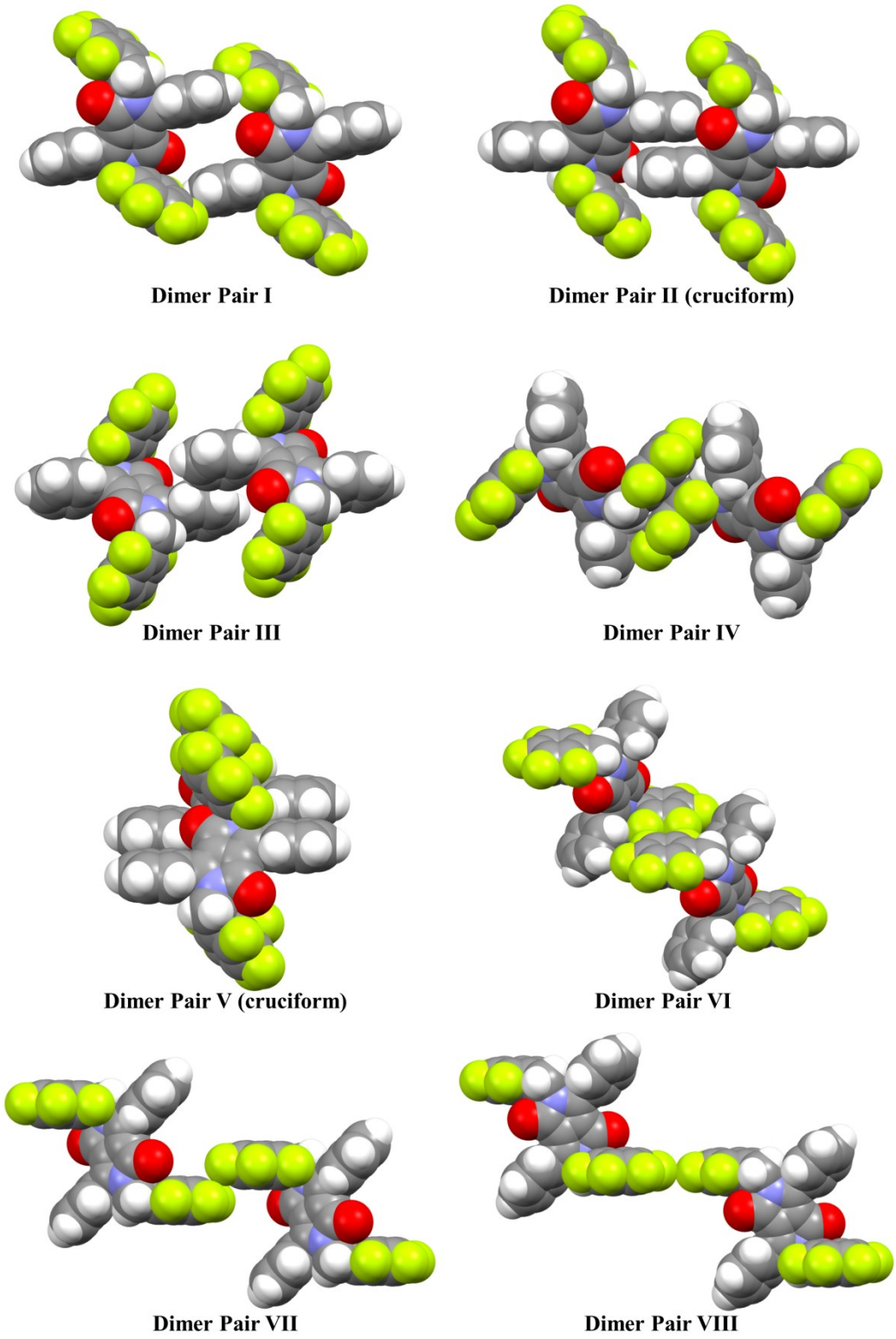

Figure 3. Space filled representation of all the nearest neighbour dimer pairs of ***HHFBDPP***.

The identified nearest neighbour dimer pairs extracted from the single crystal structure of ***HHFBDPP*** are presented in Figure 3. The role of pentafluorobenzyl (FB) substitution in these environments was investigated by producing a series of systematically cropped dimer pairs (**DPP** in Table 2) and computing their interaction energies, in line with our previous studies,[29-31] where the fluorine substituted benzyl groups were cropped and substituted with hydrogen atoms to generate their pigment-type equivalents. These results are summarised in Table 2.

Table 2. Counterpoise corrected intermolecular interactions energies, ΔE_{CP} for structurally modified and non-structurally modified dimer pairs of all the nearest neighbours of ***HHFBDPP***. M06-2X/6-311G(d)

ΔE_{CP} / KJ mol^{-1}	**Dimer pair**							
	I	**II (cruciform)**	**III**	**IV**	**V (cruciform)**	**VI**	**VII**	**VIII**
XYZBDPP	-9.64	-41.08	-1.55	-30.23	-56.17	-6.87	-3.62	-0.37
DPP	-1.95	-35.74	-1.34	-0.22	-25.25	0.26	0.72	0.19

Analysis of the computed intermolecular interactions reveals very small (ΔE_{CP} = -41.08 and -35.74 kJ mol^{-1} for **XYZBDPP** and **DPP** of dimer pair II respectively) pentafluorobenzyl induced stabilisation of the dimer pair II. The latter is associated to a weak intermolecular interaction between the electropositive para phenylic hydrogen atoms and the electron deficient pentafluorophenyl rings. In turn, most of the computed binding energy can be associated to the quasi-eclipsed π-π interaction between the DPP core phenyl rings and an electrostatic interaction

between the electronegative carbonyl oxygen and the electropositive meta phenylic hydrogen atoms located 2.542 Å apart (Figure 4). This is consistent with the computed pentafluorobenzyl induced stabilisation of the meta-fluorinated analogue, ***HFFBDPP*** (ΔE_{CP} = -22.46 and -16.75 kJ mol^{-1} for **XYZBDPP** and **DPP** of the π-π dimer pair of ***HFFBDPP*** respectively),[29] which we attribute to their similar intermonomer displacements along the short and long molecular axes as illustrated in Figure 1.

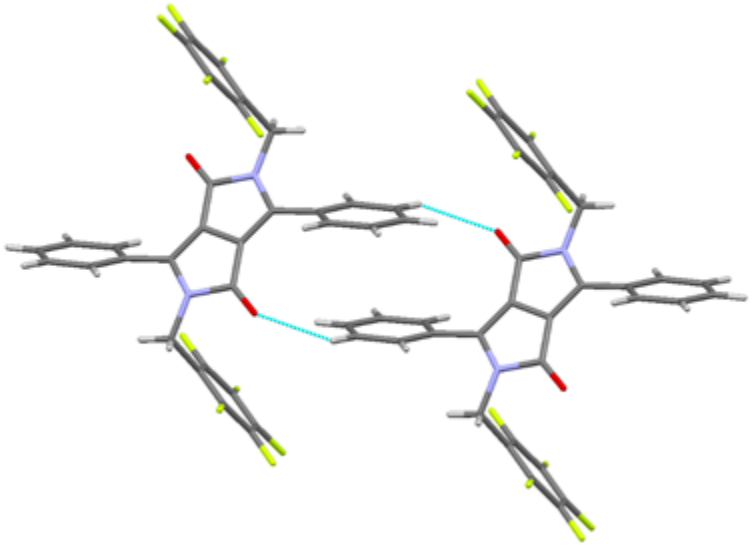

Figure 4. Capped stick representation of π-π stacking dimer pair II of ***HHFBDPP***, with illustrated close interatomic contacts.

Unlike the fluorinated species ***HHFBDPP*** and ***HFFBDPP***, the non-fluorinated analogue, ***HHHBDPP*** is characterised by a substantial destabilisation on removal of the benzyl groups (ΔE_{CP} = -70.10 and -41.90 kJ mol^{-1} for **XYZBDPP** and **DPP** of π-π dimer pair of ***HHHBDPP*** respectively). This greater benzyl induced stabilisation for the π-π dimer pair of ***HHHBDPP*** is attributed to a close electrostatic intermolecular interaction between the electropositive

methylene hydrogens and electronegative carbonyl oxygen atoms, which is precluded in the fluorinated systems given the larger shift along the long molecular axis (Δx = 4.52, 9.13 and 9.12 Å for π-π dimer pairs of ***HHHBDPP***, ***HHFBDPP*** (II) and ***HFFBDPP*** respectively)[29,30] as illustrated in Figure 5.

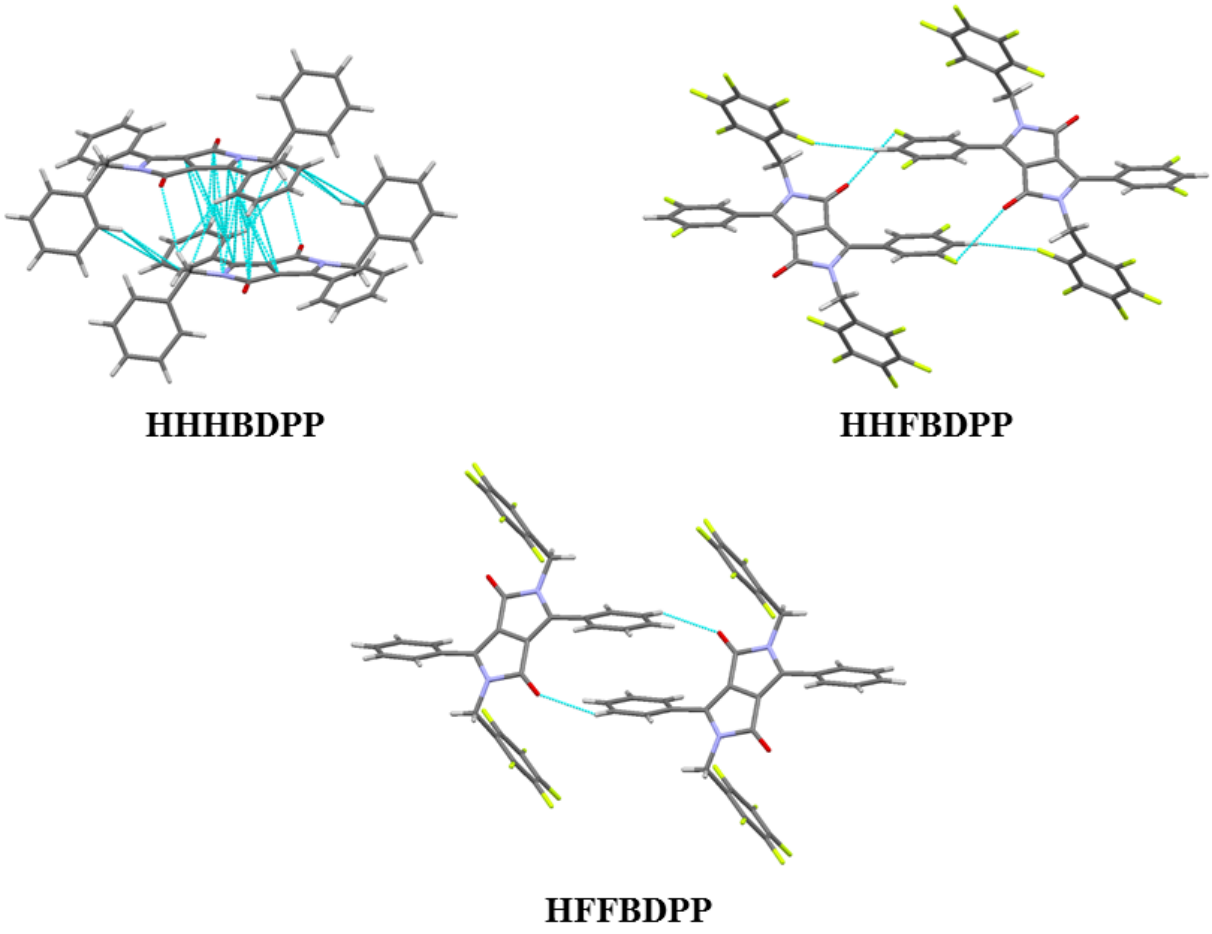

Figure 5. Capped stick representation of π-π stacking dimer pairs of ***HHHBDPP***, ***HHFBDPP*** (dimer pair II) and ***HFFBDPP***, with illustrated close interatomic contacts for each dimeric interaction.

In contrast to π-π dimer pair II in ***HHFBDPP***, the π-π stacking dimer pair V, which is characterised by significant displacement along the short molecular axis was observed to exhibit

a larger pentafluorobenzyl induced stabilisation (ΔE_{CP} =-56.17 and -25.25 kJ mol^{-1} for **XYZBDPP** and **DPP** of dimer pair V respectively). We associate this two-fold stabilisation to intermolecular interactions involving a slipped-cofacial[67-69] contact between the electron deficient pentafluorinated phenyl rings and two different electrostatic intermolecular interactions between the electronegative carbonyl oxygen of one monomer and the electropositive methylene and ortho phenylic hydrogen atoms of the other monomer, which are separated by 3.106 and 2.423 Å respectively (Figure 6).

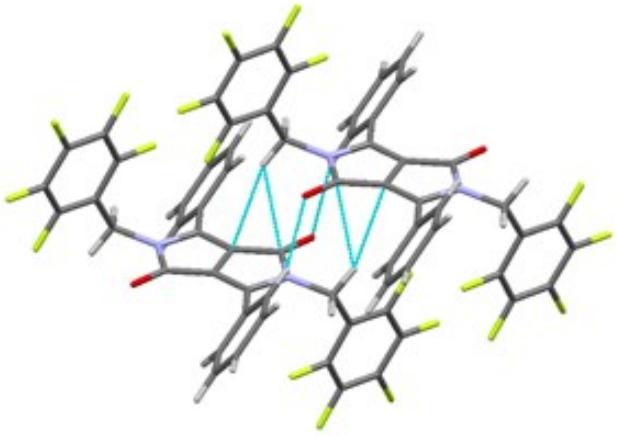

Figure 6. Capped stick representation of π-π stacking dimer pair V of ***HHFBDPP***, with illustrated close interatomic contacts.

For the remaining dimer pairs of ***HHFBDPP*** (see Figure 7), we observed a predominance of pentafluorobenzyl induced stabilisation in all cases, which was evaluated via direct comparison of the **XYZBDPP** and **DPP** dimer pairs. Of significance, was the ca. 30 kJ mol^{-1} destabilisation observed upon removal of the benzyl groups in dimer pair IV (ΔE_{CP} =-30.23 and -0.22 kJ mol^{-1} for **XYZBDPP** and **DPP**), rationalised through the loss of intermolecular interactions involving a slipped-cofacial[67-69] contact between the perfluorinated benzylic phenyl rings as previously described for dimer pair V, a T-shape interaction[70-82] between the para fluorine atoms and the

DPP core phenyl rings and to a lesser extent a close intermolecular contact of 3.209 Å between the electropositive methylene hydrogens and electronegative fluorine atoms as illustrated in Figure 7. Finally, dimer pairs I and VI were also observed to involve substantial pentafluorobenzyl induced stabilisation, which was identified by the significant reduction in their computed ΔE_{CP} on progression from **XYZBDPP** to **DPP** (ΔE_{CP} = -9.64/-1.95 and -6.87/0.26 kJ mol^{-1} for **XYZBDPP**/**DPP** for dimer pairs I and VI respectively). In the case of dimer pair I the stabilisation is ascribed to an electrostatic interaction between electronegative fluorine atoms and electropositive phenylic hydrogens (Figure 7). The pentafluorobenzyl induced stabilisation of dimer pair VI is illustrated in Figure 3 and associated to an intermolecular interaction between fluorine atoms within the benzyl groups. In summary, for this system, it is apparent that the fluorine derived interactions, although generally weak, play an important role in the stabilisation of the nearest neighbour dimer pairs, thus reinforcing our previous assertion of their important influence in structurally related DPP based motifs.

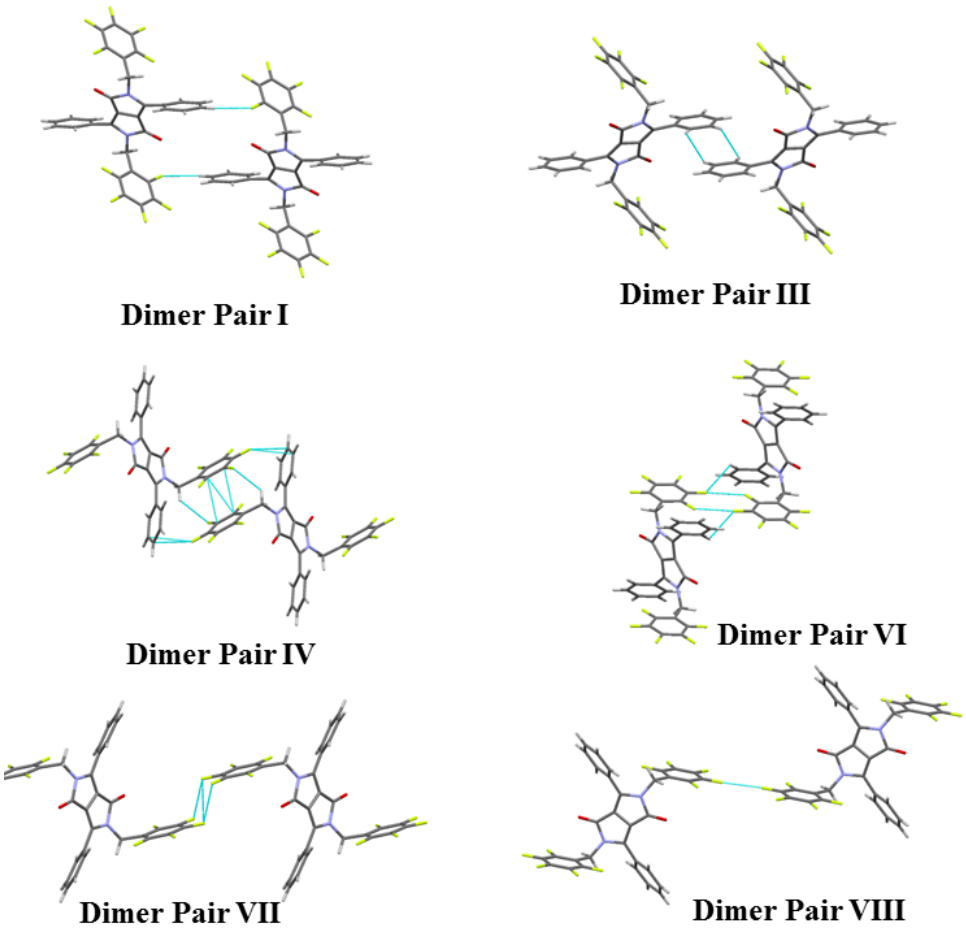

Figure 7. Capped stick representations of nearest neighbour dimer pairs I, III, IV, VI, VII and VIII of ***HHFBDPP***, with illustrated close interatomic contacts.

Charge transfer integrals, $t_{h/e}$. It is well known that small intermonomer displacements in cofacial π-π stacking dimer pairs can result in dramatic variation of computed charge transfer properties and therefore control over the effects of systematic substitutions on the charge transfer properties of π-conjugated materials is one of the major challenges in the supramolecular design of organic semiconductors. Given our interest in the rational design and development of single crystal/crystalline thin film π-conjugated organic charge transfer mediating materials, the remainder of this study focuses on the computation and analysis of hole and electron charge

transfer integrals for each of the identified dimer pairs of ***HHFBDPP.*** Hole (t_h) and electron (t_e) transfer integrals were computed for all of the centrosymmetric dimers within the framework of the energy in dimer splitting method[35] where t_h and t_e are computed as half the splitting between the corresponding supramolecular orbitals, HOMO/HOMO(-1) and LUMO/LUMO(+1) respectively. In light of the very small charge transfer integrals computed for dimer pairs I, III, IV, VI, VII and VIII (SI 2) we focus in the following on those computed for the cruciform π-π stacking dimer assemblies II and V (Figure 2).

Theoretical hole and electron transfer integrals for the π-π stacking dimer pairs II and V were determined to be t_h/t_e = 0.27/0.79 kJ mol^{-1} and t_h/t_e = 3.47/5.12 kJ mol^{-1} respectively. Based upon these crystal extracted dimer geometries we would therefore predict ambipolar charge transport behaviour from ***HHFBDPP***, with this single crystal structure favouring electron transport, via either π-π stacking domain, with more efficient electron transport occurring along the crystallographic *a*-axis, corresponding to the stacking direction of dimer pair V. Greater overall charge transport in the π-π stacking direction of dimer pair V compared with dimer pair II is consistent with their respective intermolecular interaction energies and can be accounted for on the basis of the increased long molecular axis slip and diminished wavefunction overlap observed in dimer pair II. Charge transfer integrals for the π-π dimer pairs of the non-fluorinated (***HHHBDPP***)[30] and meta fluorinated (***HFFBDPP***)[31] analogues have been reported by us previously (t_h/t_e of 10.70/6.10 and 2.01/0.89 kJ mol^{-1} respectively). In contrast to the π-π stacking dimers reported for both ***HHHBDPP*** and ***HFFBDPP***, where more favourable hole transport was predicted, fluorination of the N-benzyl phenyl groups, accompanied with no halogen substitution on the DPP core phenyl rings affords complete switching of the preferred carrier type in ***HHFBDPP***. This surprising change of behaviour can be rationalised on account of the

associated dimer geometries in each of the crystal structures and their effective wavefunction overlap, which for dimer pair V in ***HHFBDPP***, is controlled by the unusual short molecular axis slip observed in the π-π stack. Whilst the predicted electron transport behaviour of ***HHFBDPP*** does not supersede that determined for ***HHHBDPP***[30] it does approach that computed by us for rubrene (t_e = 7.46 kJ mol^{-1})[26]. Given the additional favourable impact that may be expected on the overall electron affinity of ***HHFBDPP*** as a result of fluorination, we anticipate that this DPP system could be an interesting electron transport material that should be investigated further. In addition, unlike DPP single crystal structures reported by us previously, orthogonal charge transport may be expected for ***HHFBDPP***, albeit to a lesser extent along the crystallographic *b*-axis associated with the direction of π-π stacking in dimer pair II. Therefore, despite lower hole and electron integrals compared with ***HHHBDPP***, this structure might be expected to demonstrate more effective overall charge transport in thin film based devices, owing to the enhanced dimensionality of charge transport pathways available, particularly in the presence of grain boundaries that may arise during device fabrication.

To investigate the role of the pentafluorobenzyl substitution in controlling the electronic coupling and charge carrier type in this system, we computed transfer integrals for artificially generated dimer geometries as extracted from the single crystal structure of ***HHFBDPP***, where the pentafluorobenzyl groups were removed and replaced with hydrogen atoms. Negligible differences were observed for the computed charge transfer integrals of dimer pair II on removal of the pentafluorobenzyl groups (Δt_h = 0.02 and Δt_e = 0.03 kJ mol^{-1}), which is in line with previous N-benzyl substituted systems reported by us.[30,31] In turn, a reduction in the hole transfer integral (Δt_h = 2.76 kJ mol^{-1}) and to a lesser extent the electron transfer integral (Δt_e = 0.29 kJ mol^{-1}) were computed upon removal of the fluorinated N-substituents in dimer pair V. Inspection

of the supramolecular orbitals illustrated in Figure 8 leads us to conclude that the observed decrease in t_h on progression from ***HFFBDPP*** to **DPP** is associated to a weaker bonding/anti-bonding interaction of the HOMO(-1)/HOMO upon removal of the pentafluorobenzyl substituents. This scenario contrasts with that observed for the computed electron transfer integrals, which remain unaltered since the LUMO surface does not extend through to the pentafluorobenzyl groups on the lactam nitrogen atoms as it does with the HOMO. It is anticipated that this effect should be limited to structurally related π-π dimer pairs characterised by large shifts along their short molecular axis, and accordingly has not been previously observed to this extent.

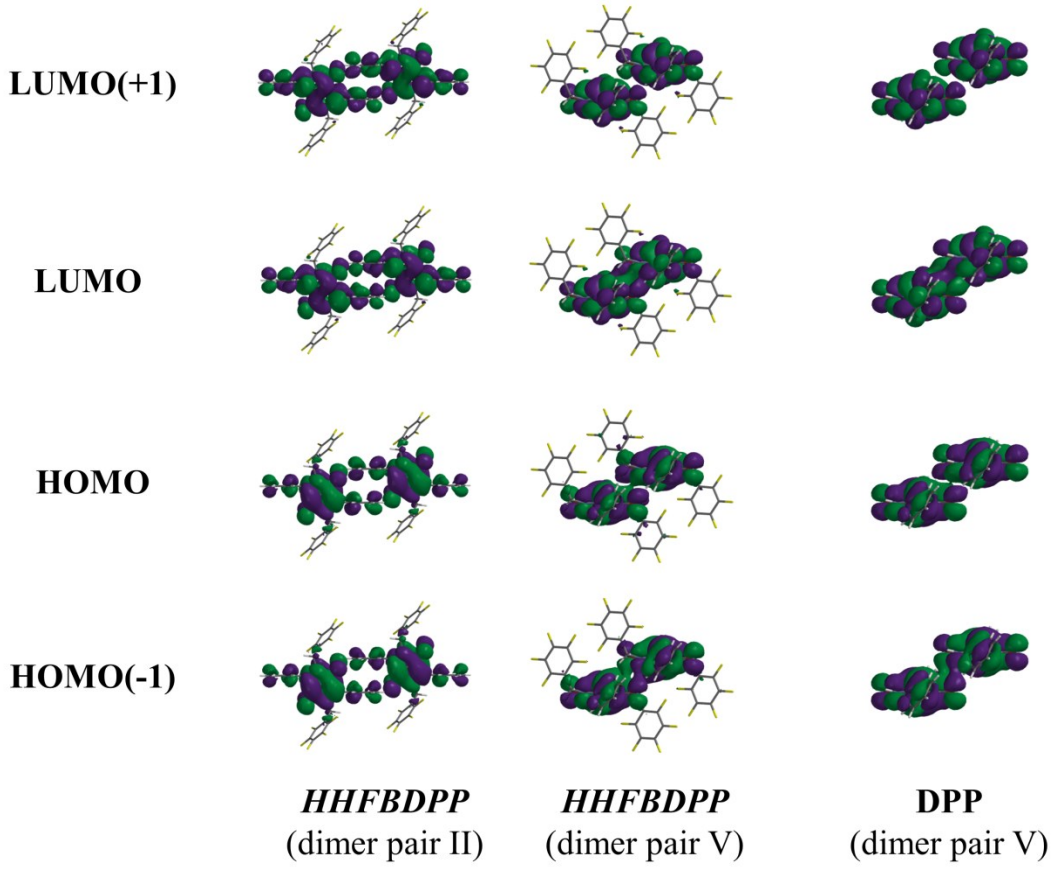

Figure 8. Illustration of the supramolecular orbitals of dimer pair II and V of ***HHFBDPP***.

CONCLUSIONS

In conclusion, we report the synthesis, characterisation and theoretical analysis of a novel fluorinated DPP based single crystal structure (***HHFBDPP***), which is characterised by the emergence of unique, 2-dimensional π-π stacking in the solid state. The structure of ***HHFBDPP*** exhibits a melting point and total intermolecular interaction energy, consistent with a larger number of nearest neighbour dimer pairs compared to its meta-fluorinated (***HFFBDPP***) and non-fluorinated (***HHHBDPP***) equivalents. Computed intermolecular interactions determined for each of the crystal derived dimer pairs of ***HHFBDPP*** and their systematically cropped equivalents were employed to investigate the role of fluorine induced stabilisation in this system. We report that, although weak, a number of intermolecular interactions involving organic fluorine (C-F---H, π_F---π and C-F---π_F) are involved in the supramolecular assembly of these dimers. In common with structural analogues reported previously, two of the dimer pairs in ***HHFBDPP*** exhibit slipped cofacial π-π stacking interactions that are characteristic of N-benzyl substitution and which are known to be crucial in the development of effective charge transfer mediating materials. One of these π-π stacking dimer pairs exhibits intermonomer displacements in line with previously reported N-benzyl substituted systems, with shifts along the long and short molecular axes that are consistent with pentafluorobenzyl substitution. To our surprise, the other π-π stacking dimer pair was significantly displaced along its short molecular axis in a cofacial dimer arrangement, which is more characteristic of non N-substituted DPP pigment analogues. The π-π stacking dimer pairs in the single crystal structure extend into mutually orthogonal 1-dimensional π-π slipped cofacial stacking motifs running the length of the *a* and *b* crystallographic axes, forming a completely unique 2-dimensional supramolecular cruciform arrangement. To the best of our knowledge, this behaviour of π-π stacking interactions has not

been reported previously and ***HHFBDPP*** represents the first example of an N-substituted DPP where high order bulk dimensionality is observed in the solid state. Charge transfer integrals for the two π-π stacking dimer pairs in ***HHFBDPP*** were determined using the energy splitting in dimer method. Ambipolar charge transport favouring electron transfer approaching that of rubrene is predicted in both of the π-π stacks with a greater magnitude of coupling observed from those dimers perpetuating along the crystallographic *a*-axis. We propose that charge transport behaviour in ***HHFBDPP*** is greatly influenced by selective fluorination of the N-benzyl substituents and is consistent with the crystal extracted π-π stacking dimer geometries and their overall influence on wavefunction overlap. Given the distinctive electronic structure of this system, heavily influenced by its unique solid state packing behaviour, we anticipate that ***HHFBDPP*** is an interesting electron transport material that should be investigated further, particularly in crystalline thin film based devices where high bulk dimensionality is desirable.

SUPPORTING INFORMATION

Position and computed hole and electron transfer integrals for each of the crystal derived dimer pairs. X-ray crystallographic information files (CIF) are available free of charge via the Internet at http://pubs.acs.org. Crystallographic information files are also available from the Cambridge Crystallographic Data Centre (CCDC) upon request (http://www.ccdc.ca.ac.uk), CCDC deposition number 1481505.

AUTHOR INFORMATION

Corresponding Authors

*E-mail: j.calvo-castro@herts.ac.uk

*E-mail: callum.mchugh@uws.ac.uk

Notes

The authors declare no competing financial interest.

ACKNOWLEDGMENT

C.J.M acknowledges the EPSRC for funding under the First Grant Scheme (EP/J011746/1) and the University of the West of Scotland for Ph.D. funding for G.M.

REFERENCES

(1) Skabara, P. J.; Arlin, J. B.; Geerts, Y. H. *Adv. Mater.* **2013**, *25*, 1948.

(2) Arumugam, S.; Wright, I. A.; Inigo, A. R.; Gambino, S.; Howells, C. T.; Kanibolotsky, A. L.; Skabara, P. J.; Samuel, I. D. W. *J. Mat. Chem. C* **2014**, *2*, 34.

(3) Wright, I. A.; Kanibolotsky, A. L.; Cameron, J.; Tuttle, T.; Skabara, P. J.; Coles, S. J.; Howells, C. T.; Thomson, S. A. J.; Gambino, S.; Samuel, I. D. W. *Angewandte Chemie - International Edition* **2012**, *51*, 4562.

(4) Kanibolotsky, A. L.; Perepichka, I. F.; Skabara, P. J. *Chem. Soc. Rev.* **2010**, *39*, 2695.

(5) Farnum, D. G.; Mehta, G.; Moore, G. G. I.; Siegal, F. P. *Tetrahedron Lett.* **1974**, 2549.

(6) Iqbal, A.; Jost, M.; Kirchmayr, R.; Pfenninger, J.; Rochat, A.; Wallquist, O. *Bull. Soc. Chim. Belg.* **1988**, *97*, 615.

(7) Wallquist, O.; Lenz, R. *Macromolecular Symposia* **2002**, *187*, 617.

(8) Herbst, W.; Hunger, K. *Industrial Organic Pigments*; Wiley-VCH, 2004.

(9) Hao, Z. M.; Iqbal, A. *Chem. Soc. Rev.* **1997**, *26*, 203.

(10) Smith, H. M. *High Performance Pigments*; Wiley-VCH, 2002.

(11) Christie, R. M. *Colour Chemistry*; The Royal Society of Chemistry, 2001.

(12) Ha, J. S.; Kim, K. H.; Choi, D. H. *J. Am. Chem. Soc.* **2011**, *133*, 10364.

(13) Cortizo-Lacalle, D.; Arumugam, S.; Elmasly, S. E. T.; Kanibolotsky, A. L.; Findlay, N. J.; Inigo, A. R.; Skabara, P. J. *J. Mater. Chem.* **2012**, *22*, 11310.

(14) Chen, Z.; Lee, M. J.; Ashraf, R. S.; Gu, Y.; Albert-Seifried, S.; Nielsen, M. M.; Schroeder, B.; Anthopoulos, T. D.; Heeney, M.; McCulloch, I.; Sirringhaus, H. *Adv. Mater.* **2012**, *24*, 647.

(15) Lee, J.; Cho, S.; Seo, J. H.; Anant, P.; Jacob, J.; Yang, C. *J. Mater. Chem.* **2012**, *22*, 1504.

(16) Hong, W.; Sun, B.; Aziz, H.; Park, W.-T.; Noh, Y.-Y.; Li, Y. *Chem. Commun.* **2012**, *48*, 8413.

(17) Liu, J.; Sun, Y.; Moonsin, P.; Kuik, M.; Proctor, C. M.; Lin, J.; Hsu, B. B.; Promarak, V.; Heeger, A. J.; Thuc-Quyen, N. *Adv. Mater.* **2013**, *25*, 5898.

(18) Bronstein, H.; Chen, Z.; Ashraf, R. S.; Zhang, W.; Du, J.; Durrant, J. R.; Tuladhar, P. S.; Song, K.; Watkins, S. E.; Geerts, Y.; Wienk, M. M.; Janssen, R. A. J.; Anthopoulos, T.; Sirringhaus, H.; Heeney, M.; McCulloch, I. *J. Am. Chem. Soc.* **2011**, *133*, 3272.

(19) Qu, S.; Wu, W.; Hua, J.; Kong, C.; Long, Y.; Tian, H. *J. Phys. Chem. C* **2010**, *114*, 1343.

(20) Qu, S.; Tian, H. *Chem. Commun.* **2012**, *48*, 3039.

(21) Qu, S.; Qin, C.; Islam, A.; Wu, Y.; Zhu, W.; Hua, J.; Tian, H.; Han, L. *Chem. Commun.* **2012**, *48*, 6972.

(22) Data, P.; Kurowska, A.; Pluczyk, S.; Zassowski, P.; Pander, P.; Jedrysiak, R.; Czwartosz, M.; Otulakowski, L.; Suwinski, J.; Lapkowski, M.; Monkman, A. P. *J. Phys. Chem. C* **2016**, *120*, 2070.

(23) Kwon, J.; Na, H.; Palai, A. K.; Kumar, A.; Jeong, U.; Cho, S.; Pyo, S. *Synth. Met.* **2015**, *209*, 240.

(24) Arumugam, S.; Cortizo-Lacalle, D.; Rossbauer, S.; Hunter, S.; Kanibolotsky, A. L.; Inigo, A. R.; Lane, P. A.; Anthopoulos, T. D.; Skabara, P. J. *ACS Applied Materials and Interfaces* **2015**, *7*, 27999.

(25) Surya, S. G.; Nagarkar, S. S.; Ghosh, S. K.; Sonar, P.; Ramgopal Rao, V. *Sensors and Actuators, B: Chemical* **2016**, *223*, 114.

(26) Homyak, P.; Liu, Y.; Liu, F.; Russel, T. P.; Coughlin, E. B. *Macromolecules* **2015**, *48*, 6978.

(27) Guo, X.; Puniredd, S. R.; He, B.; Marszalek, T.; Baumgarten, M.; Pisula, W.; Muellen, K. *Chem. Mater.* **2014**, *26*, 3595.

(28) Kanibolotsky, A. L.; Vilela, F.; Forgie, J. C.; Elmasly, S. E. T.; Skabara, P. J.; Zhang, K.; Tieke, B.; McGurk, J.; Belton, C. R.; Stavrinou, P. N.; Bradley, D. D. C. *Adv. Mater.* **2011**, *23*, 2093.

(29) Calvo-Castro, J.; Morris, G.; Kennedy, A. R.; McHugh, C. J. *Cryst. Growth Des.* **2016**, *16*, 2371.

(30) Calvo-Castro, J.; Warzecha, M.; Kennedy, A. R.; McHugh, C. J.; McLean, A. J. *Cryst. Growth Des.* **2014**, *14*, 4849.

(31) Calvo-Castro, J.; Warzecha, M.; Oswald, I. D. H.; Kennedy, A. R.; Morris, G.; McLean, A. J.; McHugh, C. J. *Cryst. Growth Des.* **2016**, *16*, 1531.

(32) Warzecha, M.; Calvo-Castro, J.; Kennedy, A. R.; Macpherson, A. N.; Shankland, K.; Shankland, N.; McLean, A. J.; McHugh, C. J. *Chem. Commun.* **2015**, *51*, 1143.

(33) Calvo-Castro, J.; McHugh, C. J.; McLean, A. J. *Dyes and Pigments* **2015**, *113*, 609.

(34) Calvo-Castro, J.; Warzecha, M.; McLean, A. J.; McHugh, C. J. *Vib. Spectrosc* **2016**, *83*, 8.

(35) Bredas, J. L.; Beljonne, D.; Coropceanu, V.; Cornil, J. *Chem. Rev.* **2004**, *104*, 4971.

(36) da Silva, D. A.; Kim, E. G.; Bredas, J. L. *Adv. Mater.* **2005**, *17*, 1072.

(37) Vura-Weis, J.; Ratner, M. A.; Wasielewski, M. R. *J. Am. Chem. Soc.* **2010**, *132*, 1738.

(38) Dhar, J.; Venkatramaiah, N.; Anitha, A.; Patil, S. *J. Mat. Chem. C* **2014**, *2*, 3457.

(39) Mizuguchi, J.; Grubenmann, A.; Rihs, G. *Acta Crystallogr. Sect. B* **1993**, *49*, 1056.

(40) Mizuguchi, J.; Miyazaki, T. *Zeitschrift Fur Kristallographie-New Crystal Structures* **2002**, *217*, 43.

(41) Mizuguchi, J.; Grubenmann, A.; Wooden, G.; Rihs, G. *Acta Crystallogr. Sect. B* **1992**, *48*, 696.

(42) Wang, J.-L.; Chang, Z.-F.; Song, X.-X.; Liu, K.-K.; Jing, L.-M. *J. Mat. Chem. C* **2015**, *3*, 9849.

(43) Yin, Q.-R.; Miao, J.-S.; Wu, Z.; Chang, Z.-F.; Wang, J.-L.; Wu, H.-B.; Cao, Y. *Journal of Materials Chemistry A* **2015**, *3*, 11575.

(44) Dunitz, J. D. *Chembiochem* **2004**, *5*, 614.

(45) Dunitz, J. D.; Taylor, R. *Chem. Eur. J.* **1997**, *3*, 89.

(46) Howard, J. A. K.; Hoy, V. J.; Ohagan, D.; Smith, G. T. *Tetrahedron* **1996**, *52*, 12613.

(47) Shimoni, L.; Glusker, J. P. *Struct. Chem.* **1994**, *5*, 383.
(48) Wang, M.; Ford, M.; Phan, H.; Coughlin, J.; Nguyen, T.-Q.; Bazan, G. C. *Chem. Commun.* **2016**, *52*, 3207.
(49) Chopra, D.; Row, T. N. G. *Crystengcomm* **2011**, *13*, 2175.
(50) Nayak, S. K.; Reddy, M. K.; Row, T. N. G.; Chopra, D. *Cryst. Growth Des.* **2011**, *11*, 1578.
(51) Berger, R.; Resnati, G.; Metrangolo, P.; Weber, E.; Hulliger, J. *Chem. Soc. Rev.* **2011**, *40*, 3496.
(52) Reichenbacher, K.; Suss, H. I.; Hulliger, J. *Chem. Soc. Rev.* **2005**, *34*, 22.
(53) Chopra, D. *Cryst. Growth Des.* **2012**, *12*, 541.
(54) Wang, C.; Dong, H.; Hu, W.; Liu, Y.; Zhu, D. *Chem. Rev.* **2011**, *112*, 2208.
(55) Sheldrick, G. M. *Acta Crystallographica Section A* **2008**, *64*, 112.
(56) Boys, S. F.; Bernardi, F. *Mol. Phys.* **2002**, *100*, 65.
(57) Zhao, Y.; Truhlar, D. G. *Theor. Chem. Acc.* **2008**, *120*, 215.
(58) Shao, Y.; Molnar, L. F.; Jung, Y.; Kussmann, J.; Ochsenfeld, C.; Brown, S. T.; Gilbert, A. T. B.; Slipchenko, L. V.; Levchenko, S. V.; O'Neill, D. P.; DiStasio, R. A., Jr.; Lochan, R. C.; Wang, T.; Beran, G. J. O.; Besley, N. A.; Herbert, J. M.; Lin, C. Y.; Van Voorhis, T.; Chien, S. H.; Sodt, A.; Steele, R. P.; Rassolov, V. A.; Maslen, P. E.; Korambath, P. P.; Adamson, R. D.; Austin, B.; Baker, J.; Byrd, E. F. C.; Dachsel, H.; Doerksen, R. J.; Dreuw, A.; Dunietz, B. D.; Dutoi, A. D.; Furlani, T. R.; Gwaltney, S. R.; Heyden, A.; Hirata, S.; Hsu, C.-P.; Kedziora, G.; Khalliulin, R. Z.; Klunzinger, P.; Lee, A. M.; Lee, M. S.; Liang, W.; Lotan, I.; Nair, N.; Peters, B.; Proynov, E. I.; Pieniazek, P. A.; Rhee, Y. M.; Ritchie, J.; Rosta, E.; Sherrill, C. D.; Simmonett, A. C.; Subotnik, J. E.; Woodcock, H. L., III; Zhang, W.; Bell, A. T.; Chakraborty, A. K.; Chipman, D. M.; Keil, F. J.; Warshel, A.; Hehre, W. J.; Schaefer, H. F., III; Kong, J.; Krylov, A. I.; Gill, P. M. W.; Head-Gordon, M. *Phys. Chem. Chem. Phys.* **2006**, *8*, 3172.
(59) Wheeler, S. E.; McNeil, A. J.; Müller, P.; Swager, T. M.; Houk, K. N. *J. Am. Chem. Soc.* **2010**, *132*, 3304.
(60) Curtis, M. D.; Cao, J.; Kampf, J. W. *J. Am. Chem. Soc.* **2004**, *126*, 4318.
(61) Mas-Torrent, M.; Rovira, C. *Chem. Rev.* **2011**, *111*, 4833.
(62) Coropceanu, V.; Cornil, J.; da Silva Filho, D. A.; Olivier, Y.; Silbey, R.; Bredas, J.-L. *Chem. Rev.* **2007**, *107*, 926.
(63) Reese, C.; Roberts, M. E.; Parkin, S. R.; Bao, Z. *Adv. Mater.* **2009**, *21*, 3678.
(64) McGarry, K. A.; Xie, W.; Sutton, C.; Risko, C.; Wu, Y.; Young, V. G., Jr.; Bredas, J.-L.; Frisbie, C. D.; Douglas, C. J. *Chem. Mater.* **2013**, *25*, 2254.
(65) Podzorov, V.; Menard, E.; Borissov, A.; Kiryukhin, V.; Rogers, J. A.; Gershenson, M. E. *Phys. Rev. Lett.* **2004**, *93*.
(66) Bredas, J. L.; Calbert, J. P.; da Silva, D. A.; Cornil, J. *Proc. Natl. Acad. Sci.U.S.A* **2002**, *99*, 5804.
(67) Wheeler, S. E.; Bloom, J. W. G. *The Journal of Physical Chemistry A* **2014**, *118*, 6133.
(68) Wheeler, S. E. *Acc. Chem. Res.* **2013**, *46*, 1029.
(69) Tauer, T. P.; Sherrill, C. D. *J. Phys. Chem. A* **2005**, *109*, 10475.
(70) Sinnokrot, M. O.; Sherrill, C. D. *J. Am. Chem. Soc.* **2004**, *126*, 7690.
(71) Parrish, R. M.; Parker, T. M.; Sherrill, C. D. *J. Chem. Theory Comput.* **2014**, *10*, 4417.

(72) Burns, L. A.; Marshall, M. S.; Sherrill, C. D. *J. Chem. Theory Comput.* **2014**, *10*, 49.
(73) Hohenstein, E. G.; Chill, S. T.; Sherrill, C. D. *J. Chem. Theory Comput.* **2008**, *4*, 1996.
(74) Antony, J.; Alameddine, B.; Jenny, T. A.; Grimme, S. *J. Phys. Chem. A* **2013**, *117*, 616.
(75) Grimme, S. *Angew. Chem. Int. Ed.* **2008**, *47*, 3430.
(76) Wheeler, S. E.; Houk, K. N. *J. Am. Chem. Soc.* **2008**, *130*, 10854.
(77) Wheeler, S. E.; Houk, K. N. *J. Chem. Theory Comput.* **2009**, *5*, 2301.
(78) Raju, R. K.; Bloom, J. W. G.; An, Y.; Wheeler, S. E. *Chemphyschem* **2011**, *12*, 3116.
(79) Wheeler, S. E. *CrystEngComm* **2012**, *14*, 6140.
(80) Parrish, R. M.; Sherrill, C. D. *J. Am. Chem. Soc.* **2014**, *136*, 17386.
(81) Sherrill, C. D. *Acc. Chem. Res.* **2013**, *46*, 1020.
(82) Sinnokrot, M. O.; Sherrill, C. D. *J. Phys. Chem. A* **2004**, *108*, 10200.

Supplementary Information for:

Fluorine directed two-dimensional cruciform π-π stacking in diketopyrrolopyrroles

Jesus Calvo-Castro,[c] Graeme Morris,[a] Alan R. Kennedy,[b] and Callum J. McHugh*[a]*

[a] School of Science and Sport, University of the West of Scotland, Paisley, PA1 2BE, UK.

[b] Department of Pure & Applied Chemistry, University of Strathclyde, Glasgow, G1 1XL, UK.

[c] School of Life and Medical Sciences, University of Hertfordshire, Hatfield, AL10 9AB, UK.

*Corresponding authors: callum.mchugh@uws.ac.uk, j.calvo-castro@herts.ac.uk

SI1. Number of equivalent dimers and site for identified stack pairs of *HHFBDPP*

Table S1.1 Number of equivalent dimers and site for different stack pairs of ***HHFBDPP***

Dimer pair	No eq. molecules	Site[a]
I	2	(3/2,1,0)
II (cruciform)	2	(1/2,1,0)
III	2	(-1/2,1,0)
IV	2	(-1/2,0,-1)
V (cruciform)	2	(-1/2,0,0)
VI	2	(2,1,1)
VII	2	(-1/2,1,1)
VIII	2	(-2,1,1)

[a] Around the monomer at (1/2,0,0)

SI2. Computed charge transfer integrals for identified dimer pairs of *HHFBDPP*

Table S2.1 Computed[a] charge transfer integrals (t_h/t_e) for different nearest neighbour dimer pairs of ***HHFBDPP***

Dimer pair	t_h / kJmol^{-1}	t_e / kJmol^{-1}
I	0.01	0.02
II (cruciform)	0.27	0.79
III	0.03	0.05
IV	0.05	0.19
V (cruciform)	3.47	5.12
VI	0.01	0.03
VII	0.01	0.00
VIII	0.00	0.00

[a] M06-2X/6-311G(d)